Contribution from the Department of Chemistry,
University of Minnesota, Minneapolis, Minnesota 55455

Cationic Polyhydride Cluster Complexes of Iridium with Chelating Diphosphine Ligands. X-ray Crystal and Molecular Structures of $[Ir_2H_5(Ph_2P(CH_2)_3PPh_2)_2]BF_4$ and $[Ir_3H_7(Ph_2P(CH_2)_3PPh_2)_3](BF_4)_2$ and Their Dynamic Nuclear Magnetic Resonance Properties

H. H. WANG and L. H. PIGNOLET*

Received December 10, 1979

Two new cationic polyhydrido cluster complexes of iridium have been synthesized and characterized by single-crystal X-ray diffraction and by ^1H and ^{31}P NMR spectroscopy. The complexes $[Ir_2H_5(dppp)_2]BF_4$ (**1**) and $[Ir_3H_7(dppp)_3](BF_4)_2$ (**2**), where dppp = 1,3-bis(diphenylphosphino)propane, are isolated in good yield from the reaction of [Ir(1,5-cyclooctadiene)(dppp)]BF_4 with H_2 in methanol solution. Crystals of both complexes were obtained. Compound **1** belongs to the $C2/c$ space group ($Z = 8$) with unit cell dimensions $a = 42.591$ (10) Å, $b = 10.798$ (3) Å, $c = 27.507$ (6) Å, and $\beta = 126.05$ (2)°, and compound **2** belongs to the $P\bar{1}$ ($Z = 2$) space group with unit cell dimensions $a = 17.525$ (9) Å, $b = 20.389$ (13) Å, $c = 13.453$ (5) Å, $\alpha = 107.16$ (4)°, $\beta = 96.42$ (4)°, and $\gamma = 89.59$ (5)°. A total of 5371 and 11284 unique reflections were used to solve the structures, and the final R values for **1** and **2** are 0.050 and 0.043, respectively. The hydride positions were not located in the crystal structure analyses. The molecular structure of **1** consists of two iridium atoms separated by 2.514 (1) Å, each possessing a nonbridging chelating dppp ligand. The hydride positions can be deduced from the structural results and from ^1H and ^{31}P NMR spectroscopy. Three doubly bridging and two terminal hydrides are present in $[(dppp)HIr(H)_3IrH(dppp)]^+$ giving approximately C_2 symmetry such that each Ir(III) center has an approximately octahedral coordination geometry, not counting the Ir–Ir interaction. The molecular structure of **2** consists of an approximately equilateral triangle of iridium atoms (average Ir–Ir distance 2.772 (1) Å) with a nonbridging chelating dppp ligand on each iridium atom such that approximately C_3 symmetry is maintained. The hydride positions can be deduced from the structural and ^1H NMR data. In acetone-d_6 solution and in the solid state, **2** possesses one triply bridging hydride, three doubly bridging hydrides, and three terminal hydrides giving approximately C_3 symmetry. As in **1**, each Ir(III) has an approximately octahedral coordination geometry. In CD_3CN solution, the structure consists of four doubly bridging hydrides and three terminal hydrides (C_1 symmetry). The NMR spectra show fluxional behavior for both complexes.

Introduction

Recent work in our laboratory has established that certain cationic complexes of rhodium(I) with chelating diphosphine ligands function as effective homogeneous catalysts for the decarbonylation of aldehydes.[1,2] As an extension of these studies, several cationic diphosphine complexes of iridium have been examined. The best rhodium catalyst for aldehyde decarbonylation is $[Rh(dppp)_2]BF_4$, where dppp = 1,3-bis(diphenylphosphino)propane.[1,2] The analogous iridium complex $[Ir(dppp)_2]BF_4$ exhibits very low catalytic activity compared with $[Rh(dppp)_2]BF_4$ for the decarbonylation of benzaldehyde.[1-3] Since this trend in activity was thought to be due to the greater basicity of the iridium complex which results in increased intermediate stability,[4] less basic mono complexes of dppp such as [Ir(COD)(dppp)]BF_4 (COD = 1,5-cyclooctadiene) and its hydrogenation products were examined. These mono complexes of dppp proved to be better decarbonylation catalysts than their rhodium analogues.[2,3] For example, [Ir(COD)(dppp)]BF_4 was considerably more active as a decarbonylation catalyst for benzaldehyde under a H_2 purge than [Rh(COD)(dppp)]BF_4.[2,3] The likely active catalytic species under these conditions are $[IrH_x(dppp)]^+$ and $[Rh(dppp)]^+$, respectively. The latter of these complexes has been studied by Baird[5] and interestingly does not form hydrido species with H_2. The analogue $[Rh(dppe)]^+$ (dppe = 1,2-bis(diphenylphosphino)ethane) has been examined by Halpern[6] and also found not to react with H_2, although it does behave as an excellent hydrogenation catalyst for olefins. The complex $[IrH_x(dppp)]^+$ has not been previously studied but a hydride species is probable in light of recent studies[7-9] and work presented in this paper. Since the iridium–mono[1,3-bis(diphenylphosphino)propane] system has not previously been studied and in light of its catalytic potential,[3,7-9] we set out to characterize the hydrogenation products of [Ir(COD)(dppp)]BF_4. Two new polyhydrido complexes were isolated in good yield from this reaction and were characterized by single-crystal X-ray analysis and by ^1H and ^{31}P NMR spectroscopy. These complexes are formulated as $[Ir_2H_5(dppp)_2]BF_4$ (**1**) and $[Ir_3H_7(dppp)_3](BF_4)_2$ (**2**). Compound

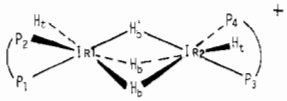

1

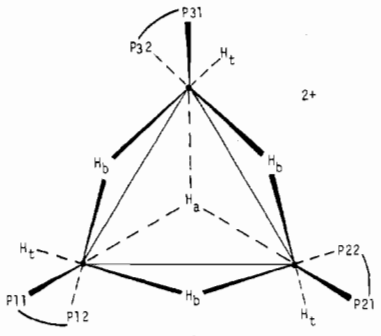

2

1 contains three doubly bridging hydrido ligands while **2** contains an unusual tricoordinate hydrido ligand within a triangle of iridium atoms. Recent interest in polyhydrido cluster complexes[7,10-12] has prompted us to report the structural

(1) Doughty, D. H.; Pignolet, L. H. *J. Am. Chem. Soc.* **1978**, *100*, 7083.
(2) Doughty, D. H.; McGuiggan, M. F.; Wang, H.; Pignolet, L. H. In "Fundamental Research in Homogeneous Catalysis"; Plenum Press: New York, 1979; Vol. 3.
(3) Wang, H.; Pignolet, L. H., results to be published.
(4) The rate-determining step in the $[Rh(dppp)_2]^+$-catalyzed decarbonylation of benzaldehyde has been shown to be phenyl group migration: Doughty, D. H. Ph.D. Thesis, University of Minnesota, 1979.
(5) Slack, D. A.; Baird, M. C. *J. Organomet. Chem.* **1977**, *142*, C69.
(6) Halpern, J.; Riley, D. P.; Chan, A. S. C.; Pluth, J. J. *J. Am. Chem. Soc.* **1977**, *99*, 8055.
(7) Crabtree, R. *Acc. Chem. Res.* **1979**, *12*, 331.
(8) Crabtree, R. H.; Felkin, H.; Morris, G. E. *J. Organomet. Chem.* **1977**, *141*, 205.
(9) Crabtree, R. H.; Felkin, H.; Fillebeen-Khan, T.; Morris, G. E. *J. Organomet. Chem.* **1979**, *168*, 183.

0020-1669/80/1319-1470$01.00/0

and dynamic NMR properties of **1** and **2**. Reactivity properties of these complexes are under current study and will be published at a later time.[3]

Experimental Section

Reagents and Solvents. Iridium trichloride hydrate was obtained from Matthey Bishop, Inc. 1,3-Bis(diphenylphosphino)propane (dppp) was purchased from Strem Chemicals and used without further purification. All solvents were reagent grade. 1,5-Cyclooctadiene was purchased from Aldrich Chemical Co. and was used without purification.

Physical Measurements. ^1H NMR spectra were recorded at 270 MHz by using a Bruker HX-270 spectrometer equipped with a Nicolet 1180 data system. Chemical shifts were referenced to internal standard tetramethylsilane and are reported in parts per million as δ values (negative values are upfield from Me_4Si). ^{31}P NMR spectra were recorded at 40.5 MHz by using a Varian Associates XL-100 FT instrument, and chemical shifts were referenced to external standard H_3PO_4. Infrared spectra were recorded on a Perkin-Elmer Model 283 spectrometer.

Synthesis of the Compounds. [Ir(dppp)(COD)]BF_4 (COD = 1,5-cyclooctadiene) was prepared by a similar route to the published synthesis of [Rh(dppp)(NBD)]BF_4 (NBD = norbornadiene).[13] The following manipulations were carried out under a purified nitrogen atmosphere by using standard Schlenk-tube techniques. $AgBF_4$ (0.43 g, 2.2 mmol) was added to an acetone solution of $[Ir(COD)Cl]_2$[14] (0.75 g, 1.1 mmol), giving an immediate white precipitate of AgCl. The slurry was refluxed for 30 min, cooled, and filtered. To the filtrate was added 25 mL of a toluene solution of dppp (0.92 g, 2.2 mmol), giving a burgandy solution. This solution was refluxed overnight, giving 1.5 g of crude product (82% yield). Recrystallization from methylene chloride–diethyl ether gave violet crystals, mp 223 °C dec. Anal. Calcd for $IrP_2C_{35}H_{38}BF_4$: C, 52.57; H, 4.79. Found: C, 52.21; H, 4.72.

[Ir_2H_5(dppp)$_2$]BF_4 (1) and [Ir_3H_7(dppp)$_3$](BF_4)$_2$ (2) were isolated as products of the same reaction. Hydrogen was slowly bubbled through ca. 10 mL of a methanol solution of recrystallized [Ir(dppp)(COD)]BF_4 at 25 °C until the burgandy color disappeared. Initially the solution turned a light yellow but gradually became a more intense yellow. Upon addition of diethyl ether, a yellow-orange precipitate formed. These manipulations were carried out under a H_2 or N_2 atmosphere so that O_2 was always excluded. Slow crystallization from methylene chloride–diethyl ether yielded crystals of pure [Ir_3H_7(dppp)$_3$](BF_4)$_2$·4CH_2Cl_2.[15] The crystals are rectangular, are intensely yellow, and readily lose solvent upon removal from the mother liquor, giving opaque crystals. IR: ν(Ir–H) 2200 cm^{-1} (br, m). Anal. Calcd for $Ir_3P_6C_{81}H_{85}B_2F_8$·$CH_2Cl_2$: C, 47.32; H, 4.31. Found: C, 47.17; H, 4.56. ^1H NMR in the hydride region at 25 °C (acetone-d_6) recorded at 270 MHz: δ – 7.98, doublet, J = 68 Hz, intensity 3; δ –8.83, quartet, J = 37 Hz, intensity 1; δ –15.0, br singlet, intensity 3. The monosolvate gave the best agreement to the analytical data. Upon addition of more diethyl ether to the mother liquor from which **2** was crystallized, additional crystals formed. These crystals were platelike, were pale yellow, and did not become opaque upon removal from the solvent. To ensure a pure product, physical separation under a microscope was necessary. This compound is [Ir_2H_5(dppp)$_2$]BF_4. IR: ν(Ir–H) = 2140 (br, s). Anal. Calcd for $Ir_2P_4C_{54}H_{57}BF_4$: C, 49.85; H, 4.42. Found: C, 49.66; H, 4.60. ^1H NMR in the hydride region at –45 °C (acetone-d_6) recorded at 270 MHz: δ –6.89, doublet, J = 70 Hz, intensity 2; δ –7.95, triplet, J = 65 Hz, intensity 1; δ –20.56, multiplet, $J \approx$ 19 Hz, intensity 2.

Collection and Reduction of X-ray Data. A summary of crystal data is presented in Table I. A crystal of **1** was secured to the end of a glass fiber with 5-min epoxy resin whereas a crystal of **2** was sealed inside of a capillary tube filled with CH_2Cl_2–heptane solution. This procedure for **2** was necessary because the crystals rapidly lost CH_2Cl_2 of crystallization and powdered. The crystal of **1** was found to belong to the *C*-centered monoclinic crystal class by the Enraf-Nonius CAD 4-SDP peak search, centering, and indexing programs and by a Dulaney reduction calculation.[16] The space group $C2/c$ was chosen from the systematic absences observed during data collection (vide infra) ($hk1$: $h + k = 2n + 1$; $h0l$: $l = 2n + 1$) and was verified by successful solution and refinement (vide infra). The crystal of **2** was found to belong to the triclinic crystal class by the methods described above, and the space group $P\bar{1}$ was verified by successful solution and refinement. Data collections were carried out on a CAD 4 Nonius diffractometer. Background counts were measured at both ends of the scan range with the use of an ω–2θ scan equal, at each side, to one-fourth of the scan range of the peak. In this manner, the total duration of measuring backgrounds is equal to half of the time required for the peak scan. The intensities of three standard reflections were measured every 1.5 h of X-ray exposure for both **1** and **2**, and no decay with time was noted. The intensities of 8934 ($\pm h,+k,+l$) unique reflections were measured at 23 °C out to 2θ of 50° using Mo Kα monochromatized radiation for **1**. The intensities of 15880 ($\pm h,\pm k,+l$) unique reflections were measured at 23 °C out to 2θ of 50° for **2**. The data were corrected for Lorentz, polarization, absorption, and background effects, using a value of 0.06 for p for both compounds.[17]

Table I. Summary of Crystal Data and Intensity Collection

compd	**1**, dimer	**2**, trimer
formula	$C_{54}H_{57}BF_4Ir_2P_4$	$C_{85}H_{93}B_2Cl_8F_8Ir_3P_6$
fw	1301.1	2326.4
a, Å	42.591 (10)	17.525 (9)
b, Å	10.798 (3)	20.389 (13)
c, Å	27.507 (6)	13.453 (5)
α, deg	90	107.16 (4)
β, deg	126.05 (2)	96.42 (4)
γ, deg	90	89.59 (5)
V, Å^3	10228	4563
Z	8	2
d(calcd), g/cm^3	1.690	1.695
space group	$C2/c$	$P\bar{1}$
cryst dimens, mm	0.30 × 0.20 × 0.10	0.30 × 0.25 × 0.25
temp, °C	23	23
radiation	Mo Kα (0.710 69 Å) from monochromator	Mo Kα (0.710 69 Å) from monochromator
linear abs factor, cm^{-1}	56.7	50.1
2θ limits, deg	0–50	0–50
final no. of variables	581	575
unique data used	5371, $F_o^2 \geq 2.5\sigma(F_o^2)$	11284, $F_o^2 \geq 3.0\sigma(F_o^2)$
R^a	0.050	0.043
$R_w{}^a$	0.059	0.060
error in an observn of unit wt	1.50	1.34

[a] The function minimized was $\Sigma w(|F_o| - |F_c|)^2$, where $w = 1/\sigma^2(F_o)$; $R = (\Sigma||F_o| - |F_c||)/\Sigma|F_o|$; $R_w = [(\Sigma w(|F_o| - |F_c|)^2/(\Sigma w|F_o|^2]^{1/2}$.

(10) Bau, R.; Teller, R. G.; Kirtley, S. W.; Koetzle, T. F. *Acc. Chem. Res.* **1979**, *12*, 176.
(11) Sivak, A. J.; Muetterties, E. L. *J. Am. Chem. Soc.* **1979**, *101*, 4878. Day, V. W.; Fredrich, M. F.; Reddy, G. S.; Sivak, A. J.; Pretzer, W. R.; Muetterties, E. L. *J. Am. Chem. Soc.* **1977**, *99*, 8091.
(12) Dedieu, A.; Albright, T. A.; Hoffmann, R. *J. Am. Chem. Soc.* **1979**, *101*, 3141.
(13) Schrock, R. R.; Osborn, J. A. *J. Am. Chem. Soc.* **1971**, *93*, 2397.
(14) Synthesized by literature method [Herde, J. L.; Lambert, J. C.; Senoff, C. V. *Inorg. Synth.* **1974**, *15*, 18] or purchased from Strem Chemicals, Inc.
(15) The tetrasolvate formula was later verified by X-ray analysis (vide infra).
(16) All calculations were carried out on PDP 8A and 11/34 computers using the Enraf-Nonius CAD 4–SDP programs. This crystallographic computing package is described in: Frenz, B. A. In "Computing in Crystallography"; Schenk, H., Olthof-Hazekamp, R., van Koningsveld, H., Bassi, G. C., Eds.; Delft University Press: Delft, Holland, 1978; pp 64–71; also "CAD 4 and SDP Users Manual"; Enraf-Nonius: Delft, Holland, 1978.
(17) The intensity data were processed as described: "CAD 4 and SDP Users Manual"; Enraf-Nonius: Delft, Holland, 1978. The net intensity $I = (K/NPI)(C - 2B)$, where $K = 20.1166x$ (attenuator factor), NPI = ratio of fastest possible scan rate to scan rate for the measurement, C = total count, and B = total background count. The standard deviation in the net intensity is given by $\sigma^2(I) = (K/NPI)^2[C + 4B + (pI)^2]$, where p is a factor used to downweight intense reflections. The observed structure factor amplitude F_o is given by $F_o = (I/Lp)^{1/2}$, where Lp = Lorentz and polarization factors. The $\sigma(I)$'s were converted to the estimated errors in the relative structure factors $\sigma(F_o)$ by $\sigma(F_o) = {}^1/_2(\sigma(I)/I)F_o$.

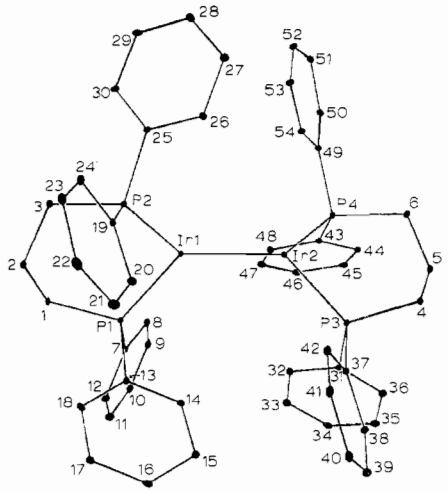

Figure 1. Drawing of the molecular structure of $[Ir_2H_5(dppp)_2]^+$ (**1**) showing the labeling scheme and the orientation of the phenyl rings.

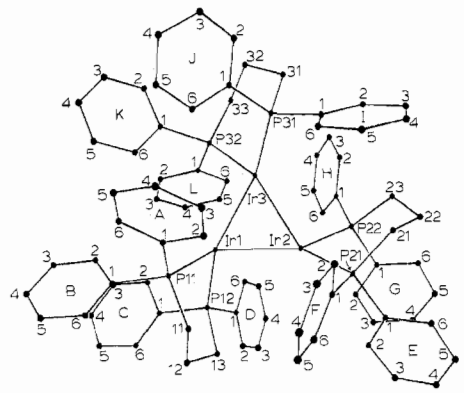

Figure 2. Drawing of the molecular structure of $[Ir_3H_7(dppp)_3]^{2+}$ (**2**) showing the labeling scheme and the orientation of the phenyl rings.

Of the 8934 unique reflections for **1**, 5371 have $F_o^2 \geq 2.5\sigma(F_o^2)$ and were used in subsequent calculations. Of the 15880 unique reflections for **2**, 11284 have $F_o^2 \geq 3.0\sigma(F_o^2)$ and were used in subsequent calculations.

Solution and Refinement of the Structures. Both structures were solved by conventional heavy-atom techniques. The Ir atoms were located by Patterson syntheses. Full-matrix least-squares refinement and difference Fourier calculations were used to locate all remaining nonhydrogen atoms.[18] The atomic scattering factors were taken from the usual tabulation,[19] and the effects of anomalous dispersion were included in F_c for Ir, P, and Cl by using Cromer and Ibers'[20] values of $\Delta f'$ and $\Delta f''$. Two tables of observed and calculated structure factors for **1** and **2** are available.[21] For **1**, all nonhydrogen atoms were refined anisotropically while for **2** only the Ir, P, F, and Cl atoms were refined anisotropically. Hydrogen atoms were not located in the final difference Fourier maps and therefore were not included, and no chemically significant peaks were observed in these maps. The final positional and thermal parameters of the atoms appear in Tables II and III. The labeling schemes for **1** and **2** are presented in Figures 1 and 2, respectively.

Results and Discussion

X-ray Structures. $[Ir_2H_5(dppp)_2]BF_4$ (1) was structurally characterized by single-crystal X-ray analysis. Relevant crystallographic data are presented in Tables I and II. The structure consists of well-separated cations and anions with no unusually short intermolecular contacts. The molecular structure of the cation is shown in Figure 1, and selected distances and angles are presented in Table IV. Figure 3 shows an ORTEP drawing of the coordination core with selected distances and angles. The shortness of the Ir–Ir distance (2.514 (1) Å) suggests significant metal–metal interaction. Indeed, this distance is one of the shortest known for iridium and very similar to the distances observed in other IrH_3Ir compounds: $[(PPh_3)_2HIrH_3IrH(PPh_3)_2]PF_6$ (**3**) (2.52 Å)[7,22] and $[(C_5Me_5)IrH_3Ir(C_5Me_5)]BF_4$ (2.458 (6) Å).[10] Since NMR data establish the presence of three bridging hydride ligands (vide infra), it is probably best to describe the bonding as three M–H–M two-electron, three-center bridge bonds.[7,11,12] The two chelating dppp groups are the only X-ray detectable ligands in the structure, and therefore each iridium appears three-coordinate with a distorted stereochemistry. The dihedral angle between the planes formed by Ir1, P1, and P2 and by Ir2, P3, and P4 is 57.9°. This is best appreciated by careful examination of the ORTEP stereoview shown in Figure 4. Clearly there are missing ligands. The 1+ charge of the cation is also established by the location of one tetrafluoroborate anion. The B and F atoms refined to give reasonable distances and angles (Table IV) considering the large thermal parameters of the F atoms and the likeliness of some disorder often found in BF_4 anions (vide infra).

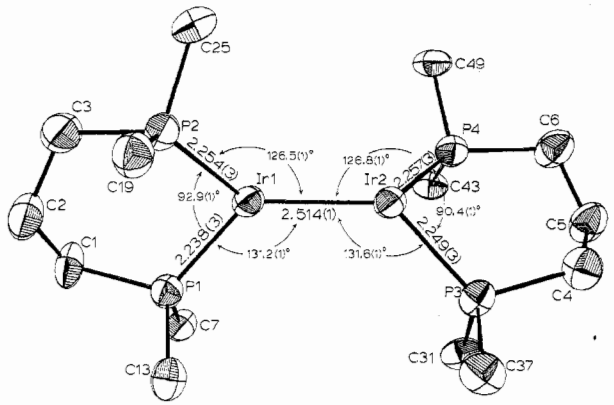

Figure 3. ORTEP drawing of **1** with selected distances and angles. The phenyl carbon atoms have been omitted for clarity, and the ellipsoids are drawn with 30% probability boundaries.

The hydride ligands were not located in the final difference Fourier, but their stereochemical positions can be inferred from the structural and NMR data. Additionally, the overall stereochemistry of **1** is quite similar to that of **3**, its PPh_3 analogue, for which the hydride positions have been inferred.[7,12] The proposed hydride positions in **1** are shown, and details of the NMR evidence for their placement will be presented in a later section. The stereochemistry about each iridium atom is therefore octahedral as expected for Ir(III). Unfortunately, the X-ray analysis of **3** was not completed due to extensive disorder,[22] so it is impossible to compare the structural differences between the dppp and $(PPh_3)_2$ analogues. The positioning of H_b' approximately trans to both the Ir1–P1 and Ir2–P3 bonds (^1H NMR −45 °C: triplet, intensity 1), the two H_b hydrides trans to Ir1–P2 and Ir2–P4, respectively (doublet, intensity 2), and the H_t hydrides trans to the H_b hydrides (multiplet, intensity 2) can be appreciated by examining the ORTEP stereoview (Figure 4). Note that the P1–Ir1 and P3–Ir2 vectors are nearly coplanar and intersect at the H_b' position. In agreement with structure **1**, the deviation of

(18) The function minimized was $\sum w(|F_o| - |F_c|)^2$, where $w = 1/\sigma^2(F_o)$. The unweighted and weighted residuals are defined as $R = (\sum ||F_o| - |F_c||)/\sum |F_o|$ and $R_w = [(\sum w(|F_o| - |F_c|))^2/(\sum w|F_o|)^2]^{1/2}$. The error in an observation of unit weight is $[\sum w(|F_o| - |F_c|)^2/(NO - NV)]^{1/2}$, where NO and NV are the number of observations and variables, respectively.
(19) Cromer, D. T.; Waber, J. T. "International Tables for X-ray Crystallography"; Kynoch Press: Birmingham, England, 1974; Vol. IV, Table 2.2.4. Cromer, D. T. *Ibid.*, Table 2.3.1.
(20) Cromer, D. T.; Ibers, J. A., in ref 19.
(21) See paragraph at end of paper regarding supplementary material.
(22) Crabtree, R. H.; Felkin, H.; Morris, G. E. *J. Organomet. Chem.* **1976**, *113*, C7.

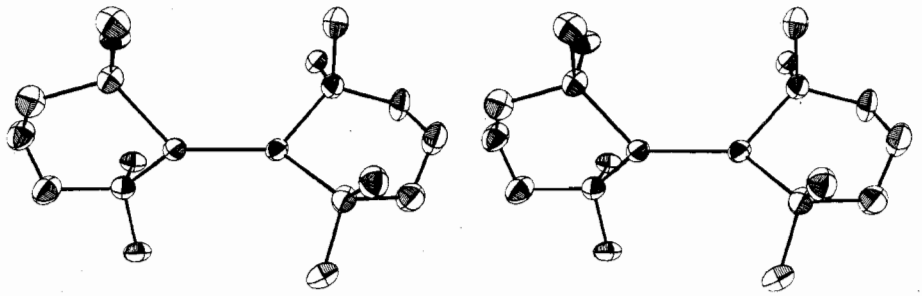

Figure 4. ORTEP stereoview of **1** with phenyl groups omitted for clarity.

Ir1 from the P1,P2,Ir2 plane and the deviation of Ir2 from the P3,P4,Ir1 plane are nonzero (0.41 and 0.44 Å, respectively).

The P–Ir–P chelate bite angles (average 91.7°) are within the range normally found for dppp complexes.[23-25] The difference between the two bite angles (92.9° vs. 90.4°), although significantly outside of experimental uncertainty (25σ), is not considered to be chemically important and probably results from crystal-packing effects. Approximate C_2 symmetry (C_2 axis passing through H_b' and the midpoint of the Ir–Ir vector) is suggested by comparing other distances and angles shown in Figure 3. NMR data are consistent with this symmetry in solution (vide infra). The Ir–P distances (average 2.250 Å) are short compared with values observed in other iridium(III) phosphine complexes (range 2.25–2.42 Å)[10,26-29] and probably reflect a combination of the low degree of steric crowding around the iridium atoms and the positive charge on the complex. Since all Ir–P bonds are trans to bridging hydrides, the four Ir–P distances should be the same. The four distances are within 0.012 Å (4σ) from the mean.

Within the dppp ligands, the phosphorus–phenyl bond distances range from 1.81 (1) to 1.84 (1) Å and average 1.83 Å, in good agreement with results from other dppp complexes.[23-25] The phosphorus–methylene linkages range from 1.83 (1) to 1.87 (1) Å and average 1.85 Å. The difference between P–C(sp^2) and P–C(sp^3) bond lengths, while of low significance, is in keeping with the variation in covalent radius of carbon with change of hybridization (i.e., ~0.77 Å for C(sp^3) and ~0.74 Å for C(sp^2)).[23] The C–P–C angles range from 99.5 (5) to 107.2 (7)° and average 103.6°. This contraction of the C–P–C angle from the tetrahedral value of 109.5° is characteristic of phosphine complexes.[30] The CH_2–CH_2 distances range from 1.52 (2) to 1.57 (1) Å and average 1.55 Å, in good agreement with the accepted C(sp^3)–C(sp^3) distance of 1.537 ± 0.005 Å.[31] The 48 carbon–carbon bonds within the phenyl rings vary from 1.35 (2) to 1.44 (2) Å and average 1.398 Å, a value which is in good agreement with the accepted C–C(aromatic) distance of 1.394 ± 0.005 Å.[32]

The Ir(III) coordination cores in **1** are six-coordinate, IrH_4P_2, and probably are distorted octahedral with no unusually short contacts between Ir and ortho-C(phenyl) atoms. The shortest distance between iridium and an ortho-carbon atom is 3.62 (2) Å for Ir2–C42, considerably longer than the distance observed where ortho-C interactions have been postulated (ca. 2.6 Å in $Rh(PPh_3)_3^+$).[33]

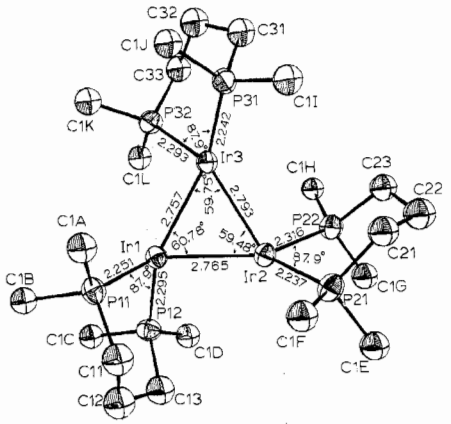

Figure 5. ORTEP drawing of **2** with selected distances and angles. The phenyl carbon atoms have been omitted for clarity, and the ellipsoids are drawn with 30% probability boundaries.

The fluorine atoms of the tetrafluoroborate anion refined with rather large thermal parameters (Table II), but a disordered model was not apparent in the final difference Fourier. The average values for the B–F distance and F–B–F angle are 1.33 (3) Å and 109 (2)°, respectively, in good agreement with accepted values.[34]

$[Ir_3H_7(dppp)_3](BF_4)_2 \cdot 4CH_2Cl_2$ (2) was structurally characterized by single-crystal X-ray analysis. Relevant crystallographic data are presented in Tables I and III. The structure consists of well-separated dications, BF_4 anions, and CH_2Cl_2 solvate molecules. The closest intermolecular contacts between the dication **2** and an anion and a solvate molecule are 3.20 Å for C31–F2 and 3.69 Å for C12–Cl6, respectively. The shortest anion–CH_2Cl_2 distance is 3.24 Å for F2–C4. The shortest intermolecular dication–dication distance is 3.46 Å between C4B and C5C. The charge of the dication is confirmed by the location and refinement of the atoms of two tetrafluoroborate anions (Tables II and VI). The molecular structure of dication **2** is shown in Figure 2 and selected distances and angles are presented in Table V. Distances and angles within the anions and solvate molecules are presented in Table VI. Figure 5 shows an ORTEP drawing of the coordination core of **2** with selected distances and angles. The molecular structure of the dication consists of an equilateral triangle of three iridium atoms with Ir–Ir separations of 2.765 (1), 2.793 (1), and 2.757 (1) Å and with triangle vertex angles of 60.78 (1), 59.48 (1), and 59.75 (1)°. Each iridium atom has a chelated dppp ligand similar to dimer **1**.

The hydride ligands have not been located by difference Fourier analysis, but their positions may be inferred (vide infra). The stereochemistry of **2** is best appreciated by examining the ORTEP stereoview presented in Figure 6. The

(23) Churchill, M. R.; Bezman, S. A. *Inorg. Chem.* **1973**, *12*, 531.
(24) Steffen, W. L.; Palenik, G. J. *Inorg. Chem.* **1976**, *15*, 2432.
(25) McGuiggan, M. F.; Doughty, D. H.; Pignolet, L. H. *J. Organomet. Chem.* **1980**, *185*, 241.
(26) Debaerdemaeker, T. *Cryst. Struct. Commun.* **1977**, *6*, 11.
(27) Clark, G. R.; Skelton, B. W.; Waters, T. N. *Inorg. Chim. Acta* **1975**, *12*, 235.
(28) Churchill, M. R.; Bezman, S. A. *Inorg. Chem.* **1974**, *13*, 1418.
(29) Roberts, P. J.; Ferguson, G. *Acta Crystallogr., Sect. B* **1976**, *32*, 1513.
(30) Churchill, M. R.; O'Brien, T. A. *J. Chem. Soc. A* **1968**, 2980.
(31) *Chem. Soc., Spec. Publ.* **1965**, *No. 18*, S14s.
(32) *Chem. Soc., Spec. Publ.* **1965**, *No. 18*, S16s.
(33) Yared, Y. W.; Miles, S. L.; Bau, R.; Reed, C. A. *J. Am. Chem. Soc.* **1977**, *99*, 7076.
(34) Cramer, R. E.; van Doorne, W.; Dubois, R. *Inorg. Chem.* **1975**, *14*, 2462.

Table II

Positional and Thermal Parameters and Their Estimated Standard Deviations for **1**[a]

atom	*x*	*y*	*z*	*B*(1,1)	*B*(2,2)	*B*(3,3)	*B*(1,2)	*B*(1,3)	*B*(2,3)
Ir1	0.16034 (1)	0.21047 (5)	0.06366 (2)	0.000 58 (0)	0.00583 (4)	0.00146 (1)	−0.00055 (2)	0.00110 (0)	−0.00043 (3)
Ir2	0.15729 (1)	−0.00342 (5)	0.02503 (2)	0.000 56 (0)	0.00608 (4)	0.00145 (1)	−0.00038 (2)	0.00106 (0)	−0.00061 (3)
P1	0.11390 (8)	0.3316 (3)	0.0526 (1)	0.000 72 (2)	0.0061 (3)	0.00173 (4)	−0.0003 (1)	0.00137 (4)	−0.0005 (2)
P2	0.20576 (8)	0.2827 (4)	0.1568 (1)	0.000 69 (2)	0.0063 (3)	0.00157 (4)	−0.0005 (2)	0.00120 (4)	−0.0008 (2)
P3	0.11119 (8)	−0.1508 (4)	−0.0136 (1)	0.000 74 (2)	0.0065 (3)	0.00147 (4)	−0.0007 (1)	0.00123 (4)	−0.0005 (2)
P4	0.17146 (8)	−0.0578 (4)	−0.0393 (1)	0.000 69 (2)	0.0069 (3)	0.00175 (4)	−0.0001 (1)	0.00136 (4)	−0.0002 (2)
F1	0.1118 (4)	0.511 (1)	0.3217 (4)	0.003 3 (1)	0.014 (1)	0.0042 (2)	−0.0016 (8)	0.0041 (2)	−0.003 (1)
F2	0.0697 (3)	0.368 (2)	0.2623 (6)	0.001 8 (1)	0.039 (2)	0.0055 (3)	−0.0106 (8)	0.0016 (3)	0.002 (2)
F3	0.0881 (4)	0.507 (1)	0.2259 (5)	0.002 5 (2)	0.026 (2)	0.0030 (2)	−0.0035 (9)	0.0011 (3)	0.007 (1)
F4	0.1279 (4)	0.368 (2)	0.2903 (7)	0.002 9 (1)	0.031 (3)	0.0097 (4)	0.0037 (10)	0.0066 (3)	−0.002 (2)
C1	0.1294 (4)	0.486 (1)	0.0885 (5)	0.001 12 (10)	0.005 (1)	0.0021 (2)	−0.0003 (7)	0.0015 (2)	−0.0021 (10)
C2	0.1654 (4)	0.489 (1)	0.1555 (5)	0.000 94 (10)	0.007 (2)	0.0019 (2)	0.0000 (7)	0.0010 (2)	−0.0020 (11)
C3	0.2044 (3)	0.451 (1)	0.1660 (5)	0.000 79 (9)	0.008 (2)	0.0022 (2)	−0.0001 (7)	0.0013 (2)	−0.0005 (11)
C4	0.1261 (3)	−0.301 (1)	−0.0251 (4)	0.000 94 (8)	0.008 (1)	0.0015 (2)	−0.0005 (6)	0.0015 (1)	−0.0013 (9)
C5	0.1356 (3)	−0.294 (1)	−0.0721 (5)	0.001 22 (8)	0.008 (2)	0.0027 (2)	−0.0015 (6)	0.0028 (1)	−0.0017 (10)
C6	0.1737 (3)	−0.228 (1)	−0.0492 (5)	0.000 98 (8)	0.009 (2)	0.0023 (2)	−0.0017 (7)	0.0019 (2)	−0.0028 (10)
C7	0.0761 (3)	0.379 (1)	−0.0254 (5)	0.000 66 (7)	0.007 (1)	0.0017 (2)	−0.0005 (5)	0.0011 (2)	−0.0005 (9)
C8	0.0838 (4)	0.380 (2)	−0.0682 (5)	0.001 31 (10)	0.009 (2)	0.0016 (2)	−0.0004 (8)	0.0017 (2)	−0.0010 (11)
C9	0.0538 (4)	0.419 (2)	−0.1276 (6)	0.001 46 (13)	0.008 (2)	0.0021 (2)	0.0004 (9)	0.0015 (2)	0.0011 (12)
C10	0.0178 (5)	0.457 (2)	−0.1432 (6)	0.001 39 (16)	0.008 (2)	0.0026 (3)	−0.0002 (9)	0.0012 (3)	0.0015 (12)
C11	0.0106 (5)	0.452 (2)	−0.0994 (7)	0.000 93 (14)	0.016 (2)	0.0035 (4)	0.0019 (10)	0.0011 (3)	0.0054 (16)
C12	0.0396 (4)	0.416 (2)	−0.0403 (6)	0.000 89 (10)	0.012 (2)	0.0030 (3)	−0.0004 (8)	0.0018 (2)	0.0021 (13)
C13	0.0859 (3)	0.261 (1)	0.0755 (4)	0.000 86 (8)	0.005 (1)	0.0017 (2)	0.0004 (5)	0.0013 (2)	0.0010 (8)
C14	0.0712 (3)	0.144 (2)	0.0525 (5)	0.000 99 (8)	0.010 (2)	0.0033 (2)	−0.0004 (7)	0.0028 (2)	−0.0002 (11)
C15	0.0493 (3)	0.075 (2)	0.0674 (5)	0.000 88 (9)	0.011 (2)	0.0028 (2)	−0.0006 (7)	0.0019 (2)	0.0007 (12)
C16	0.0432 (3)	0.133 (2)	0.1068 (5)	0.000 82 (8)	0.016 (2)	0.0029 (2)	0.0011 (8)	0.0022 (2)	0.0020 (13)
C17	0.0578 (3)	0.248 (2)	0.1306 (5)	0.000 87 (9)	0.012 (2)	0.0025 (2)	0.0010 (7)	0.0019 (2)	0.0009 (11)
C18	0.0795 (3)	0.314 (2)	0.1145 (5)	0.000 84 (8)	0.013 (2)	0.0022 (2)	0.0012 (7)	0.0019 (2)	0.0002 (11)
C19	0.2074 (3)	0.229 (1)	0.2207 (5)	0.000 83 (8)	0.006 (1)	0.0020 (2)	−0.0003 (5)	0.0016 (1)	−0.0006 (9)
C20	0.1752 (3)	0.167 (2)	0.2109 (5)	0.000 99 (9)	0.011 (2)	0.0031 (2)	0.0011 (7)	0.0024 (2)	0.0041 (11)
C21	0.1748 (4)	0.141 (2)	0.2615 (6)	0.001 50 (11)	0.015 (2)	0.0040 (2)	0.0010 (8)	0.0035 (2)	0.0069 (12)
C22	0.2061 (4)	0.172 (2)	0.3194 (6)	0.001 96 (13)	0.014 (2)	0.0037 (3)	0.0030 (9)	0.0039 (2)	0.0034 (14)
C23	0.2385 (4)	0.225 (2)	0.3285 (5)	0.002 09 (13)	0.011 (2)	0.0027 (2)	0.0003 (9)	0.0035 (2)	−0.0014 (12)
C24	0.2399 (4)	0.256 (1)	0.2789 (5)	0.001 31 (11)	0.009 (2)	0.0015 (2)	0.0005 (8)	0.0015 (2)	−0.0002 (10)
C25	0.2544 (3)	0.247 (1)	0.1790 (5)	0.000 56 (7)	0.009 (2)	0.0015 (2)	−0.0012 (5)	0.0009 (2)	0.0001 (9)
C26	0.2646 (3)	0.121 (1)	0.1852 (5)	0.000 91 (9)	0.010 (2)	0.0020 (2)	0.0012 (7)	0.0016 (2)	0.0018 (11)
C27	0.3015 (3)	0.089 (2)	0.2003 (5)	0.000 86 (9)	0.014 (2)	0.0012 (2)	0.0007 (8)	0.0010 (2)	0.0025 (11)
C28	0.3262 (4)	0.182 (2)	0.2062 (5)	0.001 14 (10)	0.016 (2)	0.0022 (2)	0.0024 (8)	0.0020 (2)	0.0027 (12)
C29	0.3163 (3)	0.303 (2)	0.2013 (6)	0.000 58 (9)	0.019 (2)	0.0022 (2)	−0.0007 (8)	0.0009 (2)	0.0030 (13)
C30	0.2791 (3)	0.340 (2)	0.1855 (5)	0.000 53 (8)	0.017 (2)	0.0018 (2)	−0.0019 (7)	0.0009 (2)	−0.0015 (12)
C31	0.0655 (3)	−0.113 (1)	−0.0865 (4)	0.000 76 (7)	0.011 (2)	0.0014 (2)	−0.0014 (6)	0.0015 (1)	−0.0007 (9)
C32	0.0553 (3)	0.011 (1)	−0.1000 (5)	0.000 83 (9)	0.010 (2)	0.0019 (2)	0.0003 (7)	0.0011 (2)	0.0020 (11)
C33	0.0199 (4)	0.039 (2)	−0.1556 (5)	0.001 22 (10)	0.017 (2)	0.0028 (2)	0.0013 (8)	0.0027 (2)	0.0037 (12)
C34	−0.0026 (3)	−0.052 (2)	−0.1951 (5)	0.000 63 (8)	0.024 (3)	0.0017 (2)	0.0011 (8)	0.0011 (2)	0.0006 (13)
C35	0.0069 (3)	−0.176 (2)	−0.1819 (5)	0.001 07 (8)	0.026 (3)	0.0018 (2)	−0.0015 (9)	0.0022 (1)	−0.0011 (12)
C36	0.0423 (3)	−0.207 (2)	−0.1258 (5)	0.000 83 (9)	0.018 (2)	0.0015 (2)	−0.0013 (8)	0.0011 (2)	−0.0011 (12)
C37	0.0962 (3)	−0.193 (1)	0.0347 (4)	0.000 86 (7)	0.008 (2)	0.0017 (2)	0.0003 (6)	0.0016 (1)	0.0013 (9)
C38	0.0584 (3)	−0.241 (1)	0.0086 (5)	0.001 09 (8)	0.011 (2)	0.0029 (2)	−0.0010 (6)	0.0027 (2)	0.0008 (10)
C39	0.0480 (4)	−0.277 (2)	0.0469 (5)	0.001 41 (9)	0.013 (2)	0.0036 (2)	−0.0012 (7)	0.0036 (2)	0.0003 (12)
C40	0.0734 (4)	−0.264 (2)	0.1073 (6)	0.002 23 (11)	0.010 (2)	0.0041 (2)	−0.0000 (8)	0.0050 (2)	−0.0001 (11)
C41	0.1111 (4)	−0.219 (2)	0.1321 (5)	0.001 83 (13)	0.008 (2)	0.0019 (2)	0.0001 (9)	0.0023 (2)	0.0013 (11)
C42	0.1220 (4)	−0.180 (1)	0.0958 (5)	0.001 37 (10)	0.008 (2)	0.0017 (2)	−0.0004 (7)	0.0020 (2)	0.0006 (9)
C43	0.1389 (3)	0.010 (1)	−0.1148 (4)	0.000 64 (7)	0.010 (1)	0.0016 (2)	0.0001 (6)	0.0012 (1)	0.0004 (9)
C44	0.1244 (3)	−0.065 (2)	−0.1669 (4)	0.000 56 (8)	0.014 (2)	0.0012 (2)	−0.0007 (7)	0.0006 (2)	−0.0003 (11)
C45	0.1006 (3)	−0.003 (2)	−0.2241 (6)	0.000 60 (8)	0.027 (3)	0.0022 (2)	−0.0017 (9)	0.0013 (2)	−0.0012 (15)
C46	0.0918 (4)	0.125 (2)	−0.2272 (6)	0.000 90 (9)	0.018 (3)	0.0027 (2)	−0.0013 (8)	0.0019 (2)	0.0019 (14)
C47	0.1059 (3)	0.190 (2)	−0.1759 (5)	0.001 04 (9)	0.015 (2)	0.0029 (2)	0.0012 (8)	0.0024 (2)	0.0044 (12)
C48	0.1290 (3)	0.134 (2)	−0.1196 (5)	0.000 92 (8)	0.011 (2)	0.0025 (2)	0.0008 (7)	0.0020 (2)	0.0018 (11)
C49	0.2193 (3)	−0.008 (1)	−0.0142 (4)	0.000 48 (6)	0.012 (2)	0.0015 (2)	−0.0005 (6)	0.0010 (1)	−0.0022 (10)
C50	0.2510 (3)	−0.035 (1)	0.0443 (5)	0.000 90 (8)	0.010 (2)	0.0027 (2)	0.0011 (6)	0.0021 (2)	0.0015 (11)
C51	0.2885 (3)	−0.001 (2)	0.0661 (5)	0.000 84 (8)	0.011 (2)	0.0028 (2)	0.0004 (7)	0.0018 (2)	−0.0022 (12)
C52	0.2939 (4)	0.074 (2)	0.0294 (6)	0.000 76 (9)	0.016 (2)	0.0033 (3)	−0.0022 (8)	0.0018 (2)	−0.0032 (15)
C53	0.2624 (4)	0.106 (2)	−0.0276 (7)	0.000 98 (10)	0.016 (2)	0.0045 (3)	−0.0018 (8)	0.0027 (2)	0.0027 (14)
C54	0.2251 (3)	0.066 (2)	−0.0499 (5)	0.000 83 (8)	0.013 (2)	0.0029 (2)	−0.0008 (7)	0.0020 (2)	0.0020 (12)
B1	0.0961 (5)	0.441 (2)	0.2721 (8)	6.5 (5)					

Root-Mean-Square Amplitudes of Thermal Vibration (Å)

atom	min	intermed	max	atom	min	intermed	max
Ir1	0.171	0.190	0.200	C32	0.198	0.236	0.270
Ir2	0.176	0.188	0.200	C34	0.191	0.217	0.375
P1	0.186	0.201	0.212	C35	0.163	0.251	0.398
P2	0.181	0.203	0.211	C36	0.191	0.235	0.326
P3	0.183	0.191	0.222	C37	0.180	0.221	0.236
P4	0.197	0.200	0.211	C38	0.177	0.268	0.278

Table II (*Continued*)

Root-Mean-Square Amplitudes of Thermal Vibration (Å)

atom	min	int med	max	atom	min	int med	max
C1	0.158	0.241	0.283	C39	0.195	0.284	0.316
C2	0.181	0.223	0.292	C41	0.191	0.233	0.346
C3	0.212	0.218	0.258	C43	0.194	0.201	0.244
C4	0.171	0.221	0.242	C44	0.164	0.213	0.287
C5	0.190	0.204	0.289	C45	0.181	0.244	0.399
C6	0.195	0.229	0.275	C46	0.208	0.254	0.346
C7	0.184	0.208	0.223	C48	0.215	0.229	0.272
C8	0.191	0.237	0.291	C49	0.167	0.184	0.273
C9	0.209	0.239	0.332	C50	0.209	0.236	0.272
C13	0.161	0.209	0.234	C51	0.204	0.239	0.297
C14	0.189	0.246	0.290	C52	0.191	0.287	0.332
C15	0.212	0.255	0.275	C54	0.190	0.253	0.302
C17	0.212	0.246	0.272	F1	0.276	0.330	0.464
C18	0.190	0.237	0.290	F2	0.230	0.383	0.592
C19	0.190	0.214	0.226	F3	0.241	0.344	0.527
C20	0.202	0.228	0.311	F4	0.348	0.461	0.508
C21	0.191	0.289	0.371	C12	0.223	0.245	0.310
C22	0.256	0.261	0.367	C30	0.166	0.235	0.322
C23	0.204	0.267	0.356	C42	0.179	0.227	0.293
C24	0.190	0.232	0.302	C47	0.208	0.242	0.329
C25	0.169	0.199	0.248	C40	0.215	0.237	0.375
C26	0.205	0.228	0.263	C33	0.210	0.263	0.335
C27	0.162	0.247	0.297	C16	0.196	0.261	0.318
C28	0.218	0.238	0.328	C53	0.190	0.300	0.369
C29	0.185	0.242	0.357	C11	0.205	0.305	0.378
C31	0.163	0.200	0.268	C10	0.203	0.247	0.356

[a] The form of the anisotropic thermal parameter is $\exp[-(B(1,1)h^2 + B(2,2)k^2 + B(3,3)l^2 + B(1,2)hk + B(1,3)hl + B(2,3)kl)]$.

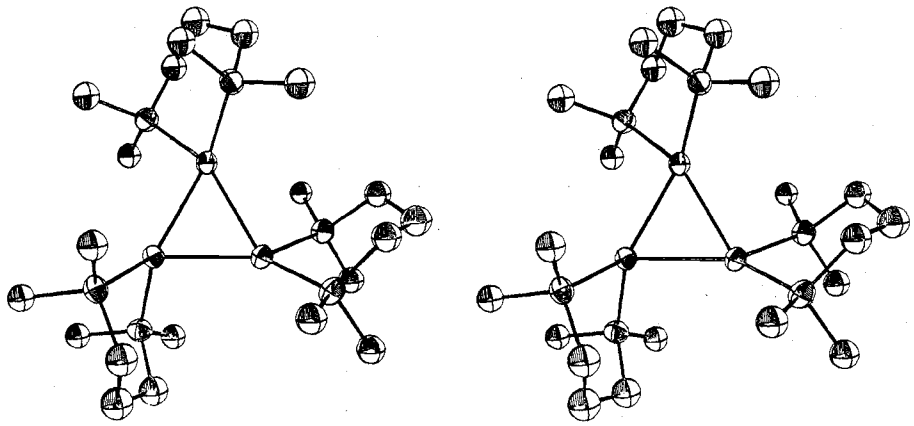

Figure 6. ORTEP stereoview of **2** with phenyl groups omitted for clarity.

molecule possesses approximate C_3 symmetry and appears to have a similar stereochemistry to $[Ir_3H_7(P\text{-}c\text{-}Hx_3)_3(C_5H_5N)_3](PF_6)_2$ (P-c-Hx$_3$ = tricyclohexylphosphine) (**4**).[35]

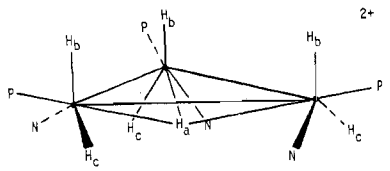

4

In both of these complexes, three P–Ir vectors (P11–Ir1, P21–Ir2, and P31–Ir3 in **2**) intersect at a position which is located approximately equidistant from the three iridium atoms—i.e., on the face of the Ir_3 triangle and on the side opposite the P11, P21, and P31 atoms. The placement of the triply bridging hydrido ligand at this position is supported by ^{1}H NMR data which shows a quartet signal for both **2** and **4**[35] (for **2**, δ −8.8, J = 37 Hz; for **4**, δ −3.9, J = 50 Hz). These NMR results are entirely consistent with a triply bridging hydride ligand (see NMR section).[35] Additional support for the similarity between **2** and **4** with respect to the triply bridging hydride stereochemistry is the closeness of the Ir–Ir separations (average values 2.772 vs. 2.765 Å for **2** and **4**, respectively) and of the average Ir–Ir–P angles (131° in **2** for P11, P21, and P31 and 136° in **4**[35]). On the assumption of reasonable Ir–H distances (ca. 1.7 Å),[10,36] the triply bridging hydride is probably 0.6–0.8 Å above or below the Ir_3 plane. The bonding is best considered a four-center, two-electron interaction.[35]

In such $M_3H_xP_6$ type complexes, the M–M–P angles can in principle be used to establish whether a trans P–M–H hydride ligand is bridging or terminal.

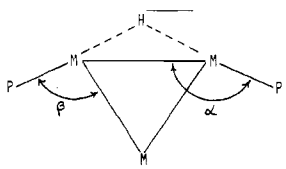

(35) Chodosh, D. F.; Crabtree, R. H. *J. Organomet. Chem.* **1978**, *161*, C67.

(36) Huie, B. T.; Knobler, C. B.; Kaesz, H. D. *J. Am. Chem. Soc.* **1978**, *100*, 3059.

Table III

Positional and Thermal Parameters and Their Estimated Standard Deviations for **2**[a]

atom	*x*	*y*	*z*	*B*(1,1)	*B*(2,2)	*B*(3,3)	*B*(1,2)	*B*(1,3)	*B*(2,3)
Ir1	0.23036 (2)	0.20745 (2)	−0.08726 (2)	0.00221 (1)	0.00167 (1)	0.00353 (2)	0.00001 (1)	0.00061 (2)	0.00178 (2)
Ir2	0.22987 (2)	0.29436 (2)	0.11397 (2)	0.00246 (1)	0.00167 (1)	0.00368 (2)	0.00041 (1)	0.00120 (2)	0.00175 (2)
Ir3	0.36732 (2)	0.24160 (2)	0.04065 (2)	0.00224 (1)	0.00161 (1)	0.00359 (2)	0.00009 (1)	0.00065 (2)	0.00145 (2)
Cl1	0.6219 (4)	0.0769 (3)	0.4033 (5)	0.0096 (3)	0.0101 (3)	0.0178 (5)	0.0011 (5)	0.0037 (7)	−0.0014 (7)
Cl2	0.7224 (5)	0.1842 (4)	0.3914 (8)	0.0178 (6)	0.0082 (3)	0.0349 (12)	0.0029 (7)	0.0084 (14)	−0.0035 (10)
Cl3	0.7253 (6)	0.4449 (4)	0.2908 (7)	0.0167 (6)	0.0241 (3)	0.0563 (7)	0.0077 (7)	0.0163 (11)	0.0617 (6)
Cl4	0.8127 (4)	0.3925 (5)	0.4330 (5)	0.0097 (3)	0.0190 (5)	0.0200 (6)	−0.0063 (6)	−0.0025 (7)	0.0154 (8)
Cl5	0.8361 (5)	0.3564 (4)	0.7776 (7)	0.0208 (6)	0.0082 (2)	0.0412 (9)	0.0016 (6)	0.0247 (11)	0.0170 (7)
Cl6	0.8815 (5)	0 2741 (5)	0.5869 (6)	0.0111 (4)	0.0258 (5)	0.0293 (7)	−0.0016 (8)	0.0036 (9)	0.0343 (8)
Cl7	0.8098 (5)	0.2247 (4)	0.1638 (7)	0.0183 (6)	0.0092 (3)	0.0291 (9)	−0.0051 (7)	0.0065 (12)	0.0043 (9)
Cl8	0.8511 (6)	0.3081 (4)	0.0383 (7)	0.0238 (7)	0.0085 (3)	0.0346 (10)	−0.0110 (7)	−0.0213 (13)	0.0146 (8)
P11	0.1971 (1)	0.2273 (1)	−0.2421 (2)	0.00291 (8)	0.00198 (5)	0.0038 (1)	−0.0003 (1)	0.0004 (2)	0.0021 (1)
P12	0.1105 (1)	0.1580 (1)	−0.1042 (2)	0.00227 (7)	0.00233 (6)	0.0051 (1)	−0.0001 (1)	0.0009 (2)	0.0029 (1)
P21	0.1938 (1)	0.4035 (1)	0.1670 (2)	0.00305 (8)	0.00191 (5)	0.0050 (1)	0.0009 (1)	0.0018 (2)	0.0020 (1)
P22	0.2614 (1)	0.3011 (1)	0.2886 (2)	0.00286 (8)	0.00220 (6)	0.0041 (1)	0.0001 (1)	0.0011 (2)	0.0022 (1)
P31	0.4803 (1)	0.2983 (1)	0.0650 (2)	0.00250 (7)	0.00202 (6)	0.0042 (1)	−0.0004 (1)	0.0004 (2)	0.0014 (1)
P32	0.4312 (1)	0.1417 (1)	−0.0199 (2)	0.00254 (7)	0.00176 (5)	0.0055 (1)	0.0007 (1)	0.0005 (2)	0.0016 (1)
F1	0.6265 (6)	0.3835 (7)	0.5452 (8)	0.0127 (5)	0.0179 (6)	0.0203 (9)	−0.0209 (8)	0.0211 (10)	−0.0252 (12)
F2	0.5792 (5)	0.3110 (4)	0.3958 (5)	0.0081 (4)	0.0066 (3)	0.0051 (4)	−0.0005 (6)	0.0032 (7)	−0.0008 (6)
F3	0.5548 (9)	0.2993 (7)	0.5401 (8)	0.0211 (9)	0.0151 (6)	0.0139 (8)	−0.0169 (10)	0.0005 (14)	0.0142 (10)
F4	0.5060 (8)	0.3746 (7)	0.5055 (10)	0.0119 (7)	0.0122 (6)	0.0212 (13)	0.0039 (11)	−0.0010 (17)	−0.0153 (15)
F5	0.8553 (9)	0.1283 (16)	−0.1889 (16)	0.0071 (7)	0.0418 (23)	0.0335 (25)	−0.0028 (22)	−0.0078 (22)	0.0107 (40)
F6	0.8022 (18)	0.1212 (8)	−0.3233 (13)	0.0557 (31)	0.0114 (6)	0.0237 (15)	−0.0013 (24)	0.0085 (37)	0.0183 (14)
F7	0.7627 (8)	0.0603 (7)	−0.2575 (14)	0.0165 (8)	0.0074 (5)	0.0496 (23)	−0.0024 (11)	0.0302 (19)	0.0028 (19)
F8	0.7545 (9)	0.1683 (8)	−0.2049 (19)	0.0148 (8)	0.0123 (6)	0.0608 (36)	0.0168 (10)	−0.0102 (29)	−0.0227 (24)

atom	*x*	*y*	*z*	*B*, Å²	atom	*x*	*y*	*z*	*B*, Å²
C11	0.1106 (6)	0.2776 (5)	−0.2347 (8)	4.5 (2)	C6F	0.1000 (7)	0.4312 (6)	0.0010 (10)	5.9 (3)
C12	0.0366 (6)	0.2375 (6)	−0.2297 (9)	5.0 (2)	C1G	0.1792 (6)	0.3050 (5)	0.3640 (7)	4.0 (2)
C13	0.0339 (6)	0.2153 (5)	−0.1269 (8)	4.4 (2)	C2G	0.1153 (6)	0.2636 (5)	0.3179 (8)	4.7 (2)
C21	0.2714 (6)	0.4578 (5)	0.2513 (7)	3.8 (2)	C3G	0.0500 (7)	0.2657 (6)	0.3736 (10)	6.1 (3)
C22	0.2883 (6)	0.4462 (5)	0.3633 (8)	4.5 (2)	C4G	0.0532 (8)	0.3111 (7)	0.4735 (11)	7.0 (3)
C23	0.3223 (5)	0.3763 (5)	0.3601 (7)	3.6 (2)	C5G	0.1130 (7)	0.3519 (6)	0.5201 (10)	6.0 (3)
C31	0.5545 (6)	0.2658 (5)	0.1458 (8)	4.1 (2)	C6G	0.1814 (6)	0.3501 (6)	0.4671 (9)	5.0 (2)
C32	0.5782 (6)	0.1930 (5)	0.0885 (8)	4.6 (2)	C1H	0.3166 (5)	0.2306 (4)	0.3189 (7)	3.1 (2)
C33	0.5146 (6)	0.1359 (5)	0.0706 (7)	3.9 (2)	C2H	0.3963 (6)	0.2365 (5)	0.3401 (8)	4.0 (2)
C1A	0.2656 (5)	0.2834 (5)	−0.2724 (7)	3.6 (2)	C3H	0.4387 (6)	0.1829 (6)	0.3641 (9)	5.1 (2)
C2A	0.2794 (7)	0.3504 (6)	−0.2040 (9)	5.2 (2)	C4H	0.4001 (7)	0.1245 (6)	0.3676 (9)	5.1 (2)
C3A	0.3298 (7)	0.3951 (6)	−0.2278 (9)	5.5 (3)	C5H	0.3215 (7)	0.1188 (6)	0.3465 (9)	5.4 (2)
C4A	0.3655 (7)	0.3746 (6)	−0.3184 (10)	5.9 (3)	C6H	0.2776 (6)	0.1717 (5)	0.3210 (8)	4.5 (2)
C5A	0.3548 (6)	0.3071 (6)	−0.3850 (9)	5.0 (2)	C1I	0.4742 (6)	0.3895 (5)	0.1347 (7)	3.9 (2)
C6A	0.3044 (6)	0.2608 (5)	−0.3634 (8)	4.1 (2)	C2I	0.4910 (6)	0.4130 (5)	0.2435 (8)	4.0 (2)
C1B	0.1821 (5)	0.1574 (4)	−0.3639 (7)	3.4 (2)	C3I	0.4840 (6)	0.4839 (6)	0.2968 (9)	4.9 (2)
C2B	0.2177 (6)	0.0955 (5)	−0.3750 (8)	4.0 (2)	C4I	0.4603 (7)	0.5277 (6)	0.2376 (9)	5.3 (2)
C3B	0.2094 (6)	0.0445 (6)	−0.4733 (9)	5.0 (2)	C5I	0.4446 (7)	0.5043 (6)	0.1280 (9)	5.5 (3)
C4B	0.1636 (7)	0.0565 (6)	−0.5574 (9)	5.1 (2)	C6I	0.4522 (6)	0.4342 (5)	0.0765 (8)	4.6 (2)
C5B	0.1296 (7)	0.1164 (6)	−0.5461 (9)	5.1 (2)	C1J	0.5279 (5)	0.2989 (5)	−0.0489 (7)	3.5 (2)
C6B	0.1354 (6)	0.1699 (5)	−0.4492 (8)	4.5 (2)	C2J	0.6043 (7)	0.3201 (6)	−0.0344 (9)	5.2 (2)
C1C	0.0939 (5)	0.0776 (5)	−0.2083 (7)	3.6 (2)	C3J	0.6428 (7)	0.3203 (6)	−0.1196 (10)	5.9 (3)
C2C	0.1481 (6)	0.0263 (5)	−0.2070 (8)	4.5 (2)	C4J	0.6043 (7)	0.2997 (6)	−0.2205 (9)	5.5 (3)
C3C	0.1397 (7)	−0.0377 (6)	−0.2862 (9)	5.8 (3)	C5J	0.5270 (6)	0.2812 (5)	−0.2339 (8)	4.8 (2)
C4C	0.0791 (8)	−0.0485 (7)	−0.3655 (10)	6.7 (3)	C6J	0.4873 (6)	0.2815 (5)	−0.1482 (8)	4.3 (2)
C5C	0.0256 (7)	−0.0002 (6)	−0.3688 (9)	5.8 (3)	C1K	0.4642 (6)	0.1195 (5)	−0.1485 (8)	4.0 (2)
C6C	0.0322 (6)	0.0642 (5)	−0.2853 (8)	4.5 (2)	C2K	0.5370 (7)	0.0917 (6)	−0.1664 (9)	5.3 (2)
C1D	0.0826 (6)	0.1304 (5)	0.0050 (7)	3.8 (2)	C3K	0.5580 (8)	0.0765 (7)	−0.2691 (10)	6.5 (3)
C2D	0.0073 (8)	0.1246 (7)	0.0173 (10)	6.4 (3)	C4K	0.5096 (8)	0.0835 (7)	−0.3518 (10)	6.4 (3)
C3D	−0.0153 (9)	0.0915 (8)	0.0936 (12)	7.8 (4)	C5K	0.4382 (7)	0.1082 (6)	−0.3368 (9)	5.7 (3)
C4D	0.0392 (7)	0.0666 (6)	0.1522 (10)	6.0 (3)	C6K	0.4159 (6)	0.1273 (5)	−0.2357 (8)	4.3 (2)
C5D	0.1156 (7)	0.0725 (6)	0.1367 (10)	6.1 (3)	C1L	0.3757 (5)	0.0666 (5)	−0.0189 (7)	3.7 (2)
C6D	0.1382 (6)	0.1047 (5)	0.0649 (8)	4.7 (2)	C2L	0.3592 (6)	0.0115 (5)	−0.1120 (8)	4.7 (2)
C1E	0.1091 (5)	0.4261 (5)	0.2355 (7)	3.8 (2)	C3L	0.3132 (7)	−0.0453 (6)	−0.1039 (10)	5.9 (3)
C2E	0.0488 (6)	0.3812 (5)	0.2201 (8)	4.5 (2)	C4L	0.2903 (7)	−0.0454 (6)	−0.0112 (10)	5.9 (3)
C3E	−0.0171 (7)	0.4022 (6)	0.2757 (9)	5.7 (3)	C5L	0.3077 (7)	0.0071 (6)	0.0803 (10)	5.8 (3)
C4E	−0.0201 (7)	0.4662 (6)	0.3404 (9)	5.7 (3)	C6L	0.3503 (6)	0.0653 (5)	0.0745 (8)	4.9 (2)
C5E	0.0382 (7)	0.5111 (6)	0.3554 (10)	6.2 (3)	C1	0.6681 (14)	0.1541 (12)	0.4853 (19)	13.6 (7)
C6E	0.1070 (6)	0.4942 (6)	0.3043 (9)	5.1 (2)	C2	0.8053 (13)	0.2925 (11)	0.6642 (17)	12.4 (6)
C1F	0.1731 (6)	0.4408 (5)	0.0582 (7)	3.9 (2)	C3	0.8119 (15)	0.2373 (13)	0.0409 (20)	15.5 (8)
C2F	0.2322 (7)	0.4900 (6)	0.0365 (10)	5.9 (3)	C4	0.7263 (13)	0.3918 (11)	0.3574 (17)	12.1 (6)
C3F	0.2131 (8)	0.5116 (7)	−0.0489 (10)	6.6 (3)					
C4F	0.1409 (8)	0.5013 (7)	−0.1000 (11)	7.3 (3)	B1	0.5718 (9)	0.3464 (8)	0.491 (1)	6.0 (3)
C5F	0.0846 (8)	0.4643 (7)	−0.0804 (11)	7.0 (3)	B2	0.7958 (14)	0.1215 (12)	−0.229 (2)	10.3 (6)

Table III (*Continued*)

Root-Mean-Square Amplitudes of Thermal Vibration (A)

atom	min	int med	max	atom	min	int med	max
Ir1	0.164	0.180	0.185	F5	0.305	0.555	0.929
Ir2	0.168	0.176	0.198	F6	0.357	0.501	0.927
Ir3	0.172	0.176	0.185	F7	0.368	0.403	0.719
P11	0.169	0.192	0.216	F8	0.274	0.482	0.920
P12	0.182	0.192	0.219	C11	0.343	0.385	0.510
P21	0.182	0.197	0.225	C12	0.356	0.525	0.608
P22	0.176	0.206	0.210	C13	0.326	0.492	0.814
P31	0.182	0.193	0.207	C14	0.355	0.405	0.618
P32	0.174	0.202	0.222	C15	0.357	0.472	0.649
F1	0.243	0.278	0.835	C16	0.387	0.418	0.717
F2	0.193	0.349	0.391	C17	0.396	0.497	0.562
F3	0.208	0.405	0.682	C18	0.352	0.441	0.718
F4	0.284	0.418	0.668				

[a] The form of the anisotropic thermal parameter is $\exp[-(B(1,1)h^2 + B(2,2)k^2 + B(3,3)l^2 + B(1,2)hk + B(1,3)hl + B(2,3)kl)]$.

Table IV. Selected Distances (Å) and Angles (Deg) in $[Ir_2H_5(dppp)_2]BF_4$ (1)

Distances (Esd)

Ir1-Ir2	2.514 (1)	P2-C19	1.81 (2)	P2-C3	1.84 (1)	P1-C7	1.84 (1)	P4-C49	1.81 (1)	C4-C5	1.57 (1)
Ir1-P1	2.238 (3)	P2-C25	1.83 (1)	P3-C4	1.83 (1)	P1-C13	1.81 (1)	P1-C1	1.85 (1)	C5-C6	1.52 (2)
Ir1-P2	2.254 (3)	P3-C31	1.84 (1)	P4-C6	1.87 (1)	P1-P2	3.256 (4)	P3-P4	3.198 (4)	B1-F1	1.34 (3)
Ir2-P3	2.249 (3)	P3-C37	1.84 (1)	C1-C2	1.56 (2)	B1-F2	1.27 (3)	B1-F3	1.32 (4)	B1-F4	1.39 (3)
Ir2-P4	2.257 (3)	P4-C43	1.84 (2)	C2-C3	1.56 (2)						

Angles (Esd)

Ir1-Ir2-P3	131.6 (1)	Ir1-P1-C1	116.5 (4)	Ir2-P3-C4	114.4 (4)	P3-Ir2-P4	90.4 (1)	Ir1-P2-C25	110.6 (5)	Ir2-P4-C49	112.6 (5)
Ir1-Ir2-P4	126.8 (1)	Ir1-P1-C7	114.7 (4)	Ir2-P3-C31	115.3 (4)	P1-C1-C2	116.2 (9)	P3-C4-C5	112.6 (9)	C1-C2-C3	114.5 (10)
Ir2-Ir1-P1	131.2 (1)	Ir1-P1-C13	114.8 (5)	Ir2-P3-C37	114.3 (6)	P2-C3-C2	110.2 (9)	P4-C6-C5	112.5 (9)	C4-C5-C6	114.2 (10)
Ir2-Ir1-P2	126.5 (1)	Ir1-P2-C3	115.0 (4)	Ir2-P4-C6	115.5 (4)	F1-B1-F2	114 (2)	F1-B1-F3	112 (2)	F1-B1-F4	99 (2)
P1-Ir1-P2	92.9 (1)	Ir1-P2-C19	120.6 (6)	Ir2-P4-C43	114.2 (5)	F2-B1-F3	116 (2)	F2-B1-F4	106 (2)	F3-B1-B4	108 (2)

Table V. Selected Distances (Å) and Angles (Deg) in $[Ir_3H_7(dppp)_3](BF_4)_2 \cdot 4CH_2Cl_2$ (2)

Distances (Esd)

Ir1-Ir2	2.765 (1)	P11-C11	1.819 (10)	P12-C13	1.833 (10)
Ir1-Ir3	2.757 (1)	P11-C1A	1.821 (8)	P12-C1C	1.816 (9)
Ir2-Ir3	2.793 (1)	P11-C1B	1.822 (8)	P12-C1D	1.836 (9)
Ir1-P11	2.251 (2)	P21-C21	1.816 (9)	P22-C23	1.827 (9)
Ir1-P12	2.295 (2)	P21-C1E	1.820 (9)	P22-C1G	1.841 (9)
Ir2-P21	2.237 (2)	P21-C1F	1.841 (9)	P22-C1H	1.846 (8)
Ir2-P22	2.316 (2)	P31-C31	1.847 (9)	P32-C33	1.822 (9)
Ir3-P31	2.242 (2)	P31-C1I	1.828 (9)	P32-C1K	1.815 (9)
Ir3-P32	2.293 (2)	P31-C1J	1.827 (8)	P32-C1L	1.823 (9)
C11-C12	1.55 (1)	C21-C22	1.59 (1)	C31-C32	1.54 (1)
C12-C13	1.58 (1)	C22-C23	1.53 (1)	C32-C33	1.57 (1)
P11-P12	3.154 (3)	P21-P22	3.159 (3)	P31-P32	3.148 (3)

Angles (Esd)

Ir2-Ir1-Ir3	60.78 (1)	Ir1-P11-C11	109.3 (3)	Ir2-P21-C1E	120.7 (3)
Ir1-Ir2-Ir3	59.48 (1)	Ir1-P11-C1A	113.2 (3)	Ir2-P21-C1F	112.8 (3)
Ir1-Ir3-Ir2	59.75 (1)	Ir1-P11-C1B	121.5 (3)	Ir2-P22-C23	112.6 (3)
Ir2-Ir1-P11	129.80 (5)	Ir1-P12-C13	112.2 (3)	Ir2-P22-C1G	115.2 (3)
Ir2-Ir1-P12	97.72 (6)	Ir1-P12-C1C	114.8 (3)	Ir2-P22-C1H	117.8 (3)
Ir3-Ir1-P11	127.80 (5)	Ir1-P12-C1D	118.5 (3)	Ir3-P31-C31	112.3 (3)
Ir3-Ir1-P12	144.32 (5)	Ir2-P21-C21	110.5 (3)	Ir3-P31-C1I	112.5 (3)
Ir1-Ir2-P21	129.25 (6)	Ir1-Ir3-P31	144.43 (5)	Ir3-P31-C1J	119.2 (3)
Ir1-Ir2-P22	142.86 (5)	Ir1-Ir3-P32	99.47 (5)	Ir3-P32-C33	111.7 (3)
Ir3-Ir2-P21	129.29 (6)	Ir2-Ir3-P31	127.09 (5)	Ir3-P32-C1K	120.1 (3)
Ir3-Ir2-P22	98.20 (5)	Ir2-Ir3-P32	143.33 (6)	Ir3-P32-C1L	112.1 (3)
P11-Ir1-P12	87.88 (8)	P21-Ir2-P22	87.87 (8)	P31-Ir3-P32	87.93 (8)
P11-C11-C12	114.3 (7)	P21-C21-C22	113.9 (6)	P31-C31-C32	111.9 (6)
C11-C12-C13	115.9 (8)	C21-C22-C23	113.6 (7)	C31-C32-C33	114.7 (7)
P12-C13-C12	114.3 (7)	P22-C23-C22	116.1 (6)	P32-C33-C32	114.8 (6)

For example, in $Rh_3H_3[P(OCH_3)_3]_6$ where the hydride positions have been shown to be doubly bridging by neutron diffraction,[11,37] the average Rh–Rh–P angles α and β are 147 and 109°, respectively, and the average Rh–Rh separation is 2.813 Å. In **2**, the average values of α and β for P12, P22, and P32 are 143 and 99°, respectively. Since the Ir–Ir separation in **2** is slightly shorter than the Rh–Rh separation (2.772 vs. 2.813 Å), the values for α and β in **2** are expected to be slightly smaller, exactly as observed. In contrast, **4** has been shown by ^1H NMR to have six terminal hydrides[35] in addition to the triply bridging hydride discussed above, and therefore the Ir–Ir–N angles α and β should be considerably smaller. This is indeed the case (α = 132°, β = 90° in **4**, Ir–Ir = 2.765 Å).[35]

The above qualitative analysis suggests that **2** possesses three doubly bridging hydrides trans to the P–Ir bonds, and by close examination of the X-ray results and the ^1H NMR results

(37) Brown, R. K.; Williams, J. M.; Fredrich, M. F.; Day, V. W.; Sivak, A. J.; Muetterties, E. L. *Proc. Natl. Acad. Sci. U.S.A.* **1979**, *76*, 2099.

Table VI. Selected Distances (Å) and Angles (Deg) in the Anions and Solvent Molecules for $[Ir_3H_7(dppp)_3](BF_4)_2 \cdot 4CH_2Cl_2$ (2)

Distances (Esd)

B1-F1	1.24 (2)	B2-F5	1.11 (3)	C1-C11	1.77 (2)
B1-F2	1.29 (2)	B2-F6	1.28 (3)	C1-C12	1.90 (2)
B1-F3	1.36 (2)	B2-F7	1.31 (3)	C2-C15	1.72 (2)
B1-F4	1.29 (2)	B2-F8	1.19 (3)	C2-C16	1.76 (2)
C3-C17	1.75 (3)	C4-C13	1.60 (2)		
C3-C18	1.62 (2)	C4-C14	1.73 (2)		

Angles (Esd)

F1-B1-F2	119 (1)	F5-B2-F6	105 (3)	C11-C1-C12	103 (1)
F1-B1-F3	108 (1)	F5-B2-F7	119 (3)	C15-C2-C16	108 (1)
F1-B1-F4	113 (1)	F5-B2-F8	117 (3)	C17-C3-C18	117 (2)
F2-B1-F3	105 (1)	F6-B2-F7	94 (2)	C13-C4-C14	113 (1)
F2-B1-F4	115 (1)	F6-B2-F8	99 (3)		
F3-B1-F4	91 (1)	F7-B2-F8	116 (3)		

(vide infra) structure **2** is proposed. This structure possesses approximate C_3 symmetry (C_3 axis is perpendicular to the Ir_3 plane and contains H_a). As required by this structure, the displacements of the P11,P21,P31 and P12,P22,P32 planes from the central Ir_3 plane are inequivalent and are 1.43 and 1.19 Å, respectively. The details of the ^1H NMR analysis, which is quite complex, will be presented in the next section; however, the room-temperature spectrum recorded in acetone-d_6 (H_a, quartet, intensity 1; H_b, doublet, intensity 3; H_t, br multiplet, intensity 3) is entirely consistent with structure **2**.

The P–Ir–P chelate bite angles in **2** range from 87.87 (8) to 87.93 (8)° and average 87.93 (8)°. This value is considerably smaller than for other dppp complexes.[23-25] The reason for the small bite angle in this complex is not known, especially since the Ir–P distances are short (average 2.272 Å) compared with those of other Ir- and Rh(dppp) complexes.[23,25] Large M–L distances usually result in small chelate bite angles; however, the P–P distance within a flexible ligand such as dppp can vary significantly and in **2** is very short (average P–P distance 3.15 Å). It is difficult to say whether steric or electronic effects are responsible for the small dppp bite angles. Interestingly, the angle observed in **2** is within the range usually observed in Ir(dppe) complexes,[24,26,38,39] and when [Ir(COD)(dppe)]BF_4 is hydrogenated at 25 °C in MeOH solution, only the trimer $[Ir_3H_7(dppe)_3]^{2+}$ is isolated.[40] With the longer backbone ligand dppb (dppb = 1,4-bis(diphenylphosphino)butane), only the dimer $[Ir_2H_5(dppb)_2]^+$ is isolated.[41] It should be noted that the P–Rh–P angles in $Rh_3H_3[P(OCH_3)_3]_6$ average 93.4°[37] while the P–Ir–N angles in **4** average 95.8°.[35]

The Ir–P distances which are trans to the triply bridging hydride range from 2.237 (2) to 2.251 (2) Å and average 2.243 Å while Ir–P distances trans to doubly bridging hydrides range from 2.293 (2) to 2.316 (2) Å and average 2.301 Å. This difference presumably results from the difference in the magnitude of the trans effect (less for triply bridging than for doubly bridging hydrides) which is well-known in hydridophosphine chemistry.[27,42] The Ir–P distances which are trans to the triply bridging hydride are among the shortest for any iridium–phosphine complex and are shorter than the ones found in dimer **1**. The weak trans effect of the triply bridging hydride ligand, the 2+ charge on the complex, and the small steric requirements about the Ir(III) centers are important factors which contribute to this short bond length.

Within the dppp ligands, the phosphorus–phenyl bond distances range from 1.815 (9) to 1.846 (9) Å and average 1.828 Å, in good agreement with results from other dppp complexes.[23-25] The phosphorus–methylene linkages range from 1.816 (9) to 1.847 (9) Å and average 1.827 Å; the C–P–C angles range from 99.2 (4) to 106.9 (4)° and average 103.5°; the CH_2–CH_2 distances range from 1.53 (1) to 1.59 (1) and average 1.56 Å. These distances and angles within the dppp chelates are similar to those found in **1** and within the range of other dppp complexes.[23-25] The phenyl rings are all planar within experimental error and have no unusual distances or angles.

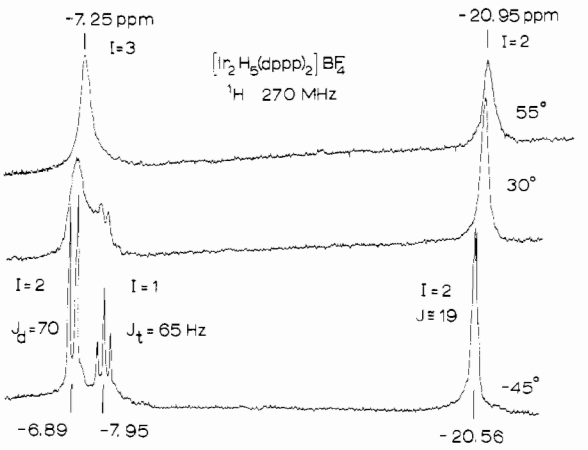

Figure 7. ^1H NMR spectra of $[Ir_2H_5(dppp)_2]BF_4$ recorded by using acetone-d_6 solvent at 270 MHz. Chemical shifts are reported as δ values with negative shifts upfield from internal standard Me_4Si.

The Ir(III) coordination cores in **2** are six-coordinate, IrP_2H_4, and probably are distorted octahedral with no unusually short contacts between Ir and phenyl C atoms (shortest distance is 3.74 Å for Ir_3–C6J). The overall geometry of **2** can be better appreciated by a consideration of the dihedral angles between certain planes. The planes formed by the IrPP chelate rings (Ir1,P11,P12; Ir2,P21,P22; Ir3,P31,P32) have dihedral angles of 63, 61, and 50°, respectively, with the plane of the Ir_3 triangle. The planes of the triangles P11,P21,P31 and P12,P22,P32 make dihedral angles of 4 and 1°, respectively, with the Ir_3 plane. Therefore, the approximate C_3 symmetry of **2** is clearly evident.

The tetrafluoroborate anions showed large thermal parameters for the fluorine atoms (Table III), and some disorder is probably present. Since the anisotropic model used gave reasonable distances and angles and an obvious disordered alternative was not apparent in the final difference Fourier, refinement was stopped at the present level. For the two tetrafluoroborate anions, the average values for the B–F distances and F–B–F angles are 1.26 Å and 108°, respectively, in reasonable agreement with accepted values.[34] The four CH_2Cl_2 solvate molecules refined to give an average C–Cl distance of 1.73 Å and an average Cl–C–Cl angle of 110°, in reasonable agreement with accepted values.[43]

NMR Spectra. $[Ir_2H_5(dppp)_2]BF_4$ (1) was examined by ^1H NMR spectroscopy at 270 MHz in the hydride region. The spectra were recorded by using acetone-d_6 solvent at several temperatures and are reproduced in Figure 7. The spectra show fluxional behavior, and the slow-exchange limit is reached at ca. −45 °C where the resonances of the nonequivalent hydride ligands shown in **1** are distinct. Chemical shifts are reported as δ values in ppm with negative shifts upfield from internal standard Me_4Si. The doublet (δ −6.89, J = 70 Hz, intensity 2) results from the two bridging hydrides H_b which are trans to a single phosphorus (^{31}P, 100%, spin = $^1/_2$) atom; the triplet (δ −7.95, J = 65 Hz, intensity 1) results from the bridging hydride H_b' which is trans to two equivalent phos-

(38) Churchill, M. R.; Bezman, S. A. *Inorg. Chem.* **1973**, *12*, 260.
(39) Goldberg, S. Z.; Eisenberg, R. *Inorg. Chem.* **1976**, *15*, 58.
(40) Preliminary results from C. Tso.
(41) Preliminary results from H. Wang.
(42) Orioli, P. L.; Vaska, L. *Proc. Chem. Soc., London* **1962**, 333.
(43) Cowie, M.; Haymore, B. L.; Ibers, J. A. *Inorg. Chem.* **1975**, *14*, 2617.

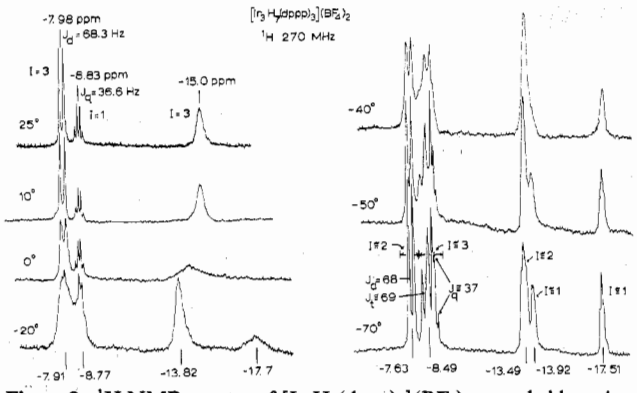

Figure 8. ^1H NMR spectra of $[Ir_3H_7(dppp)_3](BF_4)_2$ recorded by using acetone-d_6 solvent at 270 MHz.

phorus atoms P1 and P3; the multiplet (δ −20.56, $J \approx 19$ Hz, intensity 2) results from the terminal hydrides H_t which show cis phosphorus coupling. H–H coupling in metal hydrides is very small ($J_{HH} < 10$ Hz) and rarely is observed.[44] All of the observed spin–spin coupling in this complex results from P–H interaction, and the J_{PH} values are as expected for the proposed bonding modes. $J_{PH(cis)}$ coupling constants are normally in the range 10–30 Hz while $J_{PH(trans)}$ couplings are normally in the range 130–180 Hz for terminal hydrides.[44,45] The observed $J_{PH(trans)}$ coupling constants of 70 and 65 Hz are in the range expected for bridging hydrides where reduced bond orders are present.[7,11,22,35] The PPh_3 analogue **3** has a very similar ^1H NMR spectrum (−90 °C, acetone-d_6) (δ −6.9, doublet, J = 86 Hz, intensity 2; δ −8.4, triplet, J = 65, intensity 1; δ −23.9, multiplet, $J \simeq 18$, intensity 2).[7,22] As the temperature is increased, the bridging hydrides H_b and H_b' exchange rapidly on the NMR time scale, causing coalescence of the triplet and doublet signals (Figure 7). A similar process has been observed in **3**.[22] Note that at these temperatures the bridge and terminal hydride do not show signs of exchange on the NMR time scale.

An important observation is the relative chemical-shift values of the bridging and terminal hydrides in **1** and **3**. The bridging hydrides resonate at lower field (δ −6 to −9) than the terminal hydride (δ −20 to −24). This is contrary to numerous other polyhydrido cluster compounds where the bridging hydride resonances are at higher field than the terminal ones.[44] Clearly this trend cannot be generalized and must be used with caution. In the known polyhydrido clusters which contain only phosphine[7,22,35] or phosphite[11] ligands, however, the bridging hydride resonances are found at lower fields than terminal ones, and this observation should be useful in assigning the spectrum of the trimer **2**.

The variable temperature $^{31}P\{^1H\}$ NMR spectra recorded at 40.5 MHz of **1** show dynamic behavior consistent with the proposed structure. At 25 °C a broad resonance is observed (δ(P) 0.9 relative to external H_3PO_4) which splits into two complex multiplets separated by approximately 2 ppm. This behavior is qualitatively similar to that observed for **3**.[22]

$[Ir_3H_7(dppp)_3](BF_4)_2$ (2) has been examined by ^1H NMR spectroscopy at 270 MHz by using acetone-d_6 and CD_3CN solvents. The spectra obtained by using acetone-d_6 solvent show complex fluxional behavior and are reproduced in Figure 8. At 25 °C the spectrum can be assigned to structure **2** in a seemingly straightforward manner: a doublet at δ −7.98 (J = 68 Hz, intensity 3) results from the three bridging hydrides H_b which are trans to one phosphorus atom, a quartet at δ −8.83 (J = 37, intensity 1) results from the triply bridging hydride H_a which is trans to three equivalent phosphorus atoms, and a broad peak at δ −15.0 (intensity 3) results from the three terminal hydrides H_t which are cis to two phosphorus atoms. This assignment assumes C_3 symmetry and is consistent with the X-ray structural results (vide supra). The magnitude of the J_{PH} coupling constants is consistent with this assignment, and the bridge and terminal hydrides resonate in the chemical shift ranges found in **1** and **3** (vide supra).

Before discussion of the low-temperature spectra, a comparison to compound **4** will be made. Compound **4** has a considerably different ^1H NMR spectrum and does not exhibit fluxional behavior.[35] The proposed structure for **4** has been shown, and its ^1H NMR assignments are as follows: H_a, quartet, δ −3.9 (J = 50 Hz, intensity 1); H_b, doublet, δ −20 (J = 25, intensity 3); H_c, doublet, δ −22 (J = 10, intensity 3).[35] The only common feature between **2** and **4** is the presence of a quartet resonance in the downfield region since both compounds are proposed to have a triply bridging hydride ligand trans to three equivalent phosphorus atoms. The other resonances in **4** are due to terminal hydrides which have $J_{PH(cis)}$ and chemical shift values in the range expected for this assignment. It is surprising that **4** does not exhibit fluxional behavior in light of the dynamic behavior observed for **2** (Figure 8).

The fluxional behavior of **2** is complex, and if **2** is the only NMR observable species in solution, the heptahydride formulation is uncertain. Indeed, the resonance assigned to the terminal hydride region (δ −15.0 at 25 °C) splits into three resonances (δ −13.49, −13.92, −17.51) with relative intensities ca. 2:1:1, respectively. This coalescence pattern requires at least four terminal hydride ligands on one compound or the presence of isomers which rapidly interconvert above 0 °C. The relative intensities in the 25 °C spectrum (3:1:3) which have been determined several times by using different instrumental conditions seem to rule out the possibility of four terminal hydrides. The presence of several isomers which rapidly interconvert above 0 °C and which do not permit fast bridge–terminal hydride exchange seems to us to be the only tenable assignment. The remainder of the ^1H NMR coalescence behavior is at least qualitatively consistent with this model; however, better resolved spectra recorded at a higher field strength are required for a less ambiguous assignment. Careful examination of the spectra shown in Figure 8 reveals that as the temperature is lowered to −70 °C the doublet resonance at 25 °C (δ −7.98, J = 68 Hz) splits into a new doublet (δ −7.63, J = 68) and a complex pattern (possibly a triplet or two doublets) not well-resolved due to overlap with the quartet resonance. The complex pattern is centered at δ −8.49 and has $J \approx 69$ Hz. The quartet resonance (δ −8.83, J = 37) is distinct above 0 °C and appears to be present in the −70 °C spectrum but is not well resolved. The approximate relative intensities are shown in Figure 8 for the −70 °C spectrum and seem to suggest a nonahydride complex with four terminal and five bridging hydride ligands. We have not been successful at constructing a stereochemical model with this formulation which is consistent with the −70 °C ^1H NMR spectrum and the dynamic behavior. The 25 °C spectrum is also inconsistent with the nonahydride formulation. Additionally, a nonahydride formulation would require the iridiums to be in +3, +4, and +4 oxidation states which is less consistent with the chemistry of **2**. For example, **2** reacts with CO and causes catalytic decarbonylation of aldehydes.[3]

The best model which can be put forth at this time and which is not inconsistent with the data at hand is the presence of two isomers of **2** which rapidly interconvert above ca. 0 °C by a process which does *not* average bridge and terminal hydrides. Two such isomers are shown in **5** and are labeled according to their symmetry types. S represents a solvent molecule. The C_1 isomer can interconvert with the C_3 isomer

(44) Kaesz, H. D.; Saillant, R. B. *Chem. Rev.* **1972**, *72*, 231.
(45) Chatt, J.; Coffey, R. S.; Shaw, B. L. *J. Chem. Soc.* **1965**, 7391.

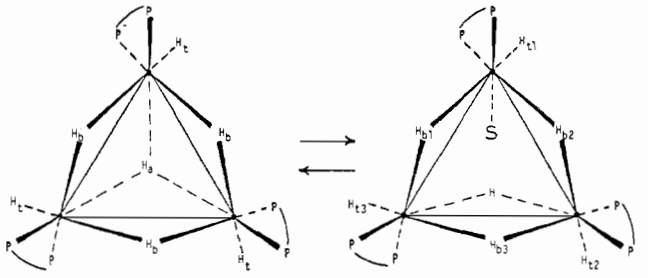

5

via movement of a hydride between the doubly bridging H and the triply bridging H_a positions. There are three equivalent ways of forming the C_1 isomer from the C_3 isomer. When the interconversion is fast, the ^1H NMR spectrum will appear as observed at 25 °C. For slow interconversion, the resonances due to both the C_1 and C_3 isomers should be present. The C_1 isomer will have three terminal hydride resonances (H_{t1}, H_{t2}, H_{t3}), and three doublets ($H_{b}1$, H_{b2}, H_{b3}) and one triplet H in the bridging region while the C_3 isomer will have the same qualitative spectrum as observed at 25 °C but with different chemical shifts. Allowing for accidental degeneracies, the observed −70 °C spectrum could result from this model; however, better resolved spectra especially in the bridging hydride region are needed for a detailed assignment.

Strong support for the presence of two isomers of **2** in acetone-d_6 solvent is provided by examination of the ^1H NMR spectrum of **2** recorded in CD_3CN solvent. The hydride region of this spectrum which was recorded at 25 °C and 270 MHz is reproduced in Figure 9. The doublet (δ −8.02, J = 67 Hz), quartet (δ −8.85, J = 36), and broad singlet (δ −15.0) resonances due to the C_3 isomer (vide supra) are clearly evident, but their intensities are small compared with the other resonances present. Seven new resonances are observed, and all have the same integrated intensity. These peaks can be assigned to an isomer of **2** which is presumably solvated by CD_3CN. The structure of such an isomer to which the ^1H NMR spectrum can be assigned is shown in **6**. The two triplet

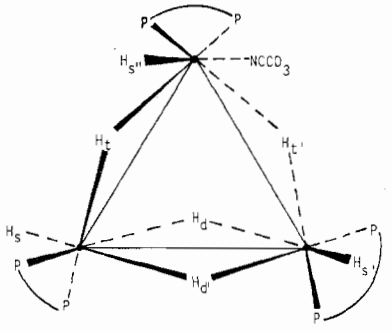

6

resonances (δ −12.61, −15.70) result from H_t and $H_{t'}$, the two doublet resonances (δ −9.28, −14.55) result from H_d and $H_{d'}$, and the three broad multiplets (δ −17.58, −21.86, −23.95) result from H_s, $H_{s'}$, and $H_{s''}$. The observed J_{PH} coupling constants and the relative resonance positions are consistent with this assignment (vide supra). Although **6** may not be the only structure giving rise to an acceptable assignment, the choices of alternate models are quite limited, and **6** is a very reasonable

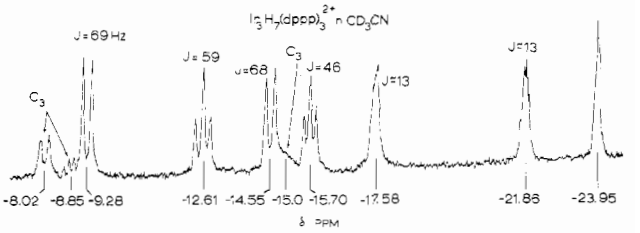

Figure 9. ^1H NMR spectrum of $[Ir_3H_7(dppp)_3](BF_4)_2$ recorded by using CD_3CN solvent at 270 MHz.

choice. The presence of the seven resonances of equal intensity provides very strong support for the heptahydride formulation of **2**. Additionally, the observation of two isomers in CD_3CN, one of which is also observed in acetone-d_6, provides good support for the interpretation of the acetone-d_6 ^1H NMR data (vide supra). The isomers shown in **5** are likely to be solvated by acetone-d_6.

A possible alternative explanation for the observed ^1H NMR behavior in acetone-d_6 could involve the presence of mononuclear or dinuclear species in equilibrium with the trimer. This is unlikely since peaks due to dimer **1** are not observed and the addition of a large excess of dppp ligand has no effect on the ^1H NMR spectra of **2** in the hydride region, suggesting that the trimer is quite robust.

The $^{31}P\{^1H\}$ NMR spectra have also been recorded for **2** in acetone-d_6 at 40.5 MHz between 25 and −60 °C. The spectra show complex fluxional behavior. At 25 °C only two resonances are present (broad singlet, δ +1.03, intensity 1; doublet, δ −7.86 vs. H_3PO_4, J = 33 Hz, intensity 1) which is consistent with structure **2** or a rapid $C_3 \rightleftharpoons C_1$ interconversion. As the temperature is lowered, the δ 1.03 resonance broadens and eventually splits into three broad multiplets. The δ −7.86 doublet also broadens and splits into three doublets ($J \approx 30$–35 Hz). The spin–spin coupling observed here is due to cis P–P coupling, and the magnitude of $J_{PP(cis)}$ is similar to published values.[46] At −60° a very complex spectrum emerges with considerable overlap of peaks extending from δ +9 to −13. The relative intensities of the six peaks cannot be accurately determined, but it appears that they do not all have the same intensity. The $^{31}P\{^1H\}$ NMR results confirm the complexity of the problem and are not inconsistent with the suggested model.

The presence of isomers for **2** suggests the possibility of disorder in the solid state. If the C_1 and C_3 isomers were both present the X-ray results might be expected to show unusual thermal parameters in the Ir_3P_6 coordination core. Examination of the data in Table III reveals no such effects, suggesting that the structure is not disordered.

Acknowledgment. Support of this research through a grant from the National Science Foundation is gratefully acknowledged. We also thank the NSF for partial support of our X-ray diffraction and structure-solving equipment (NSF Grant CHE77-28505). The Matthey Bishop Co. is acknowledged for a loan of $IrCl_3$.

Registry No. **1**, 73178-84-4; **2**, 73178-87-7; [Ir(dppp)(COD)]BF_4, 73178-89-9; $[Ir(COD)Cl]_2$, 12112-67-3.

Supplementary Material Available: Two structure factor tables (74 pages). Ordering information is given on any current masthead page.

(46) Sanger, A. *J. Chem. Soc., Dalton Trans.* **1977**, 120.